6

Synthesis and application of magnetic nanoparticles

Kishwar Khan[1], Sarish Rehman[2], Hafeez Ur Rahman[3], Qasim Khan[4]

[1]Research School of Engineering, Australian National University (ANU), Canberra, Australia
[2]College of Engineering, Peking University (PKU), Beijing, China
[3]iUSE School of Engineering, 3rd Floor, Malikabad complex, Main Murree road, Rawalpindi, Pakistan
[4]Department of Mechanical and Aerospace Engineering, Politecnico di Torino, Italy

Outline:

Introduction

Nanoparticles are key focus of research for a wide outspread novel applications, not only because of their fabulous properties, but also due to nano size compared with their bulk counterparts. Nanoparticles are intermediate between atomic and bulk level. At nano level, the properties greatly changed, as the size of the particles changed owing to their large surface to volume ratio. Owing to their wide spread applications, a lot of research has been carried out for the synthesis of 1-dimensional (1D) nano structured (nanotubes [1-4], nanorods [5-7], nanobelts [8-10], nanorings [11-14], nanohelics [15, 16], nanowires [17, 18], nanofibres [18-20], nano sphere [21-24] nano flowers [24-27] and nano sheets [28, 29] like structures.

Among nano materials magnetic nanoparticles are of keen interest to researchers owing to their praise worthy magnetic properties. Magnetic nano particles have a wide range of applications, including magnetic fluids recording [30], catalysis [31], biotechnology/biomedicine [32], material sciences, photo catalysis[33], electrochemical and bioeletrochemical sensing [34], microwave absorption [35], magnetic resonance imaging [MRI] [36], medical diagnosis, data storage [37], environmental remediation [38] and, as an electrode, for supercapictors and lithium ion batteries (LIB) [39-41]. While talking of, various magnetic nano particles, magnetite (Fe_3O_4) has been used for a several wide number of applications due to its superparamagnetic properties but one property of being sensitive to oxidation and agglomeration, has lemmatized its use. The solution to this problem is, to protect the magnetic nano particles by various types of coatings. These shells not only protect the magnetic nano particles, but, also provide a new platform for further functionalization that enhances the properties of the magnetic nano particles. Nowadays, a lot of novel binary and ternary magnetic nano composites have been synthesized with various core shell structure including grapheme [42], carbon nanotube [43, 44], conducting polymer [45], metal oxide and other inorganic materials as coating on magnetic nanoparticles [46]. Bing *et al* and co-workers have synthesized Fe_3O_4/Polyaniline hybrid microspheres for microwave absorption [35]. They used Fe_3O_4 as core material to elevate the microwave absorption properties of Polyaniline for low cost and superior electromagnetic wave absorption properties [47]. Hazhir *et al* and co-worker, reported the synthesis of Fe_3O_4/r-GO (reduced graphene oxide) nanocomposite for electrochemical sensing. The composite possesses both the electrical conductive and superparamagnetic properties due to excellent electronic, mechanical and thermal properties of graphene and superior magnetic properties of Fe_3O_4 [34]. Haijuan *et al* and co-worker, reported the synthesis of hollow Fe_3O_4/SiO_2@PEG–PLA ternary nanocomposite for targeted drug delivery. This nanocomposite have shown promising therapeutic application for its magnetic hollow silica microspheres and biodegradable nature of the polymer [48]. Peichang *et al* and co-worker have synthesized Fe_3O_4@TiO_2 core/shell nanoparticles which were supported by reduced graphene oxide sheets for excellent photocatalytic properties.

Owing to its unique and creative applications in every field of life, researcher are highly focused to develop a number of synthetic way to synthesize magnetic nanoparticles of different sizes, morphology and compositions, but the successful application of magnetic nanoparticles in the above listed application is highly dependent on the stability of the particles under a band of different conditions. The significance of size for controlling the various properties is obvious, because in most of the cases, the properties of the magnetic nano particles are dependent on their dimension, and morphology. Therefore, the synthesis of magnetic nano particles with their controlled size and exposed facets is of core importance. In most of applications, the particles with 5–15 nm sizes have unexpected excellent results, but the size requirement totally depends upon the material and applications in which they are supposed to be used. But as discussed above that the main problem associated with magnetic particles is their agglomeration which they tend to reduce the energy associated with the high surface area to

volume ratio of the nanosized particles. In addition, the magnetic nano particles are highly chemically active. Therefore it is of utmost important to protect these magnetic nano particles against oxidation, which may involve functionalization and coating with certain protective layer to form core shell structure which completely modifies the magnetic nano particles. Although modification is useful, because it provides unique properties to the core magnetic nano particle, so it can be used in a number of applications but it lead to the reduction of magnetic properties. Single crystalline magnetic nano particles have been synthesized but recently the challenge is to control their size, morphology and surface area in a precise manner to make them useful for many applications. Nowadays narrow size distribution is first priority for certain application like nano crystal based optical devices semiconductor and magnetic resonance imaging [16-20].

It has been elaborated above that the successful applications of magnetic nanoparticles in various field depends on particle size, surface area and morphology besides to their intrinsic magnetic moment and magneto crystalline anisotropy characteristics. A precise control of these various factors (size, shape, composition, and structure) can control the magnetic characteristics of the material.

Thus, this chapter describes the precise control of nanoscale magnetism, the synthesis methods of well dispersed and isolated magnetic nanoparticles with defined magneto crystalline properties. This chapter gives a concise overview of the research progress achieved in the synthesis of magnetic nano particles during the last couple of years, as well as, throws light on a few applications of magnetic nanoparticles in numerous sectors.

Synthesis

Synthesis of magnetic nanostructures

Various approaches such as wet chemical [49-51], template-directed [52, 53], microemlusion [54-56], thermal decomposition [56, 57], solvo-thermal method [58, 59], solid state [60, 61], deposition method [62], spray pyrolysis [63, 64], self-assembly [65, 66], physical and lithographic [67, 68] techniques have been extensively used for the synthesis of a wide variety of magnetic nanostructures including iron oxide, metal, metal alloys and core–shell and composites structures. However a comprehensive review of various synthetic techniques is beyond the scope of this chapter, so here we will give a short description of only those methods that offer excellent size and shape control.

Chemical synthesis

Several chemical methods that are being used for the synthesis of magnetic nanostructures comprise of co-precipitation, thermal decomposition, microemlusion and hydrothermal methods. Thermal decomposition and hydrothermal approaches provide better results (both in terms of size and morphology) in comparison with other synthetic routes [61, 69]. Chemical syhthesis involved the precipitation of nano particles from the solution. To achieve the monodisperse particles, the precipitation should comply with the LaMer and Dinegar model of homogeneous precipitation. According to this model, during precipitation from the solution at certain stage of super saturation, there occur a burst of nucleation that gradually grows in size by diffusion of solutes from the solution towards the nuclei until the monodisperse final size particle are obtained. The mechanism LaMer and Dinegar model is shown in Scheme 1.

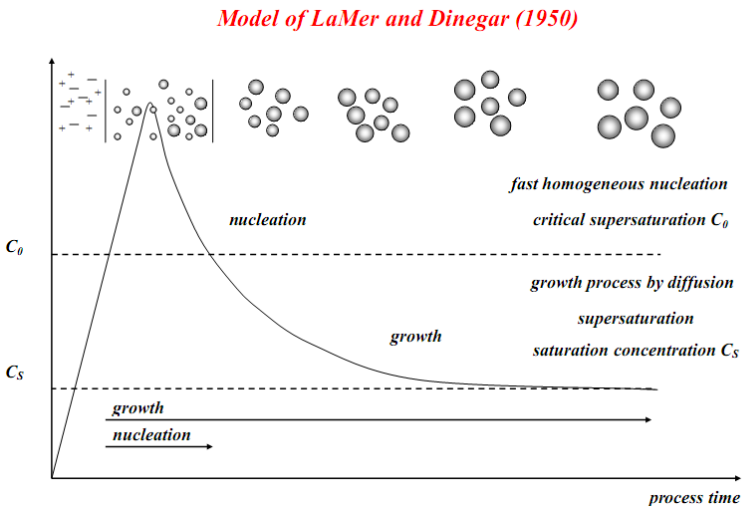

SCHEME 1
LaMer and Dinegar model of homogeneous precipitation

Some of the chemical methods are discussed below.

Thermal Decomposition

This method of synthesis involves the chemical decomposition of the substance at elevated temperature. During this method the breaking of the chemical bond takes place. This method of synthesis for magnetic nanostructures mostly use organometallic compounds such as acetylacetonates in organic solvents (benzyl ether, Ethylenediamine and carbonyls) with surfactants such as oleic acid, oleylamine, polyvinyl pyrrolidone (PVP), cetyltrimethyl ammonium bromide (CTAB) and hexadecylamine.
In this method the composition of various precursors that are involved in the reaction determine the final size and morphology of the magnetic nanostructures. Peng *et al* and co-workers used the thermal decomposition approach for controlled synthesis (in term of size and shape) of magnetic oxide [70]. Using this methods nanocrystals with very narrow-sized distribution (4–45 nm) could be synthesized along with the excellent control of morphology (spherical particles, cubes).

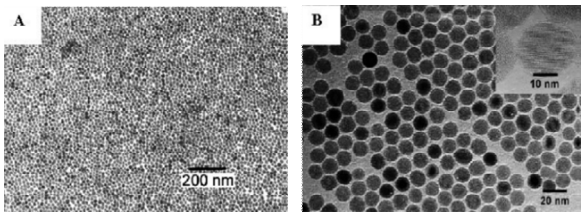

FIGURE 6.1
Maghemite nanoparticles prepared by thermal decomposition of Iron precursors: (*a*) FeCup3 (*b*) $Fe(CO)_5$ Reprint from Ref [71]

When thermal decomposition method is used, iron oxide nano particles with excellent control of size, morphology and good crystallinity have been resultantly fabricated by Alivisatos and co-workers [71]. The preparation of magnetic nanoparticles for applications in biomedicine have fabricated maghemite nanocrystals with size of 3-9 nm by thermal decomposition of FeCup3 (Cup: *N*-nitrosophenylhydroxylamine) at 250° C-300° C as shown in **Fig 6.1**. Recently, Sun and Zeng *et al* [72] have demonstrated the fabrication of monodisperse magnetite nanoparticles with size ranges of 2-20nm by decomposition of iron (III) acetyl acetone at 260°C in the presence of benzyl ether, oleic acid and oleyl amine. In a more recent study, Nogues and co-workers have synthesized highly mono disperse cubic and spherical maghemite (Fe_2O_3) nanocrystals by using thermal decomposition method [73] as shown in **Fig 6.2**.The ratio of precursors and the thermal decomposition time can be used to achieve size and morphology controlled nanocrystals.

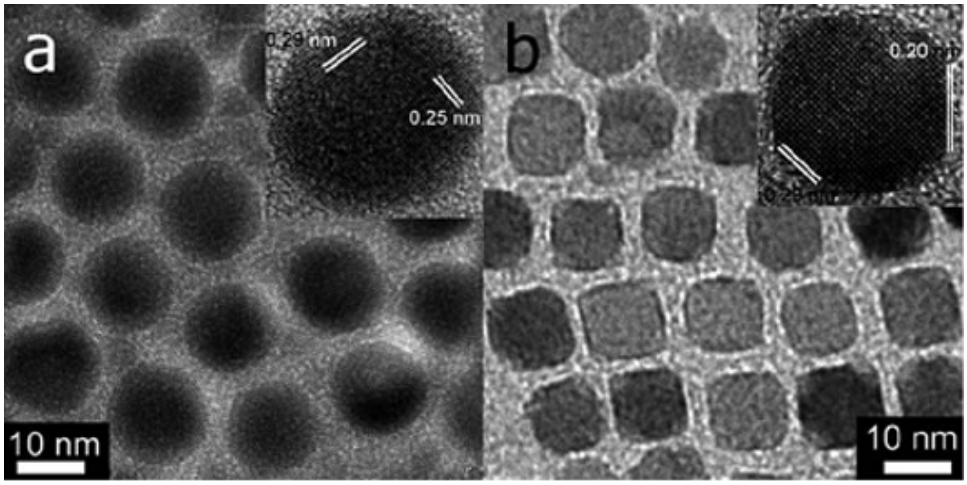

FIGURE 6.2
High resolution TEM images showing the mono disperse (a) nanosphere and (b) nanocubes achieved by thermal decomposition method. Re printed from ref [73]

It has been observed from Nogues and co-workers research that short decomposition duration (2-4 hr) resulted in spherical whereas longer duration (10-12hr) resulted in cubic morphology. The technique of thermal decomposition was not only used for synthesis of metal oxide magnetic nanocrystals but metal magnetic nanoparticles of 3d transition metals (Co, Ni, Fe) were also synthesized through introducing a reducing agent into a hot solution of metal precursor and surfactant [74]. With the precise control of temperature and the ratio of metal precursor to surfactant the magnetic nano particles with control size and shape have been synthesized.

Hydrothermal Synthesis

Another important chemical synthesis technique that involves the use of liquid–solid–solution (LSS) reaction and gives excellent control over the size and shape of the magnetic nano particles is the hydrothermal synthesis. This method involves the synthesis of magnetic nano particles from high boiling point aqueous solution at high vapor pressure. It is a unique approach for the fabrication of metal, metal oxide [75, 76], rare earth transition metal magnetic nanocrystals [77], semi-conducting [78], dielectric, rare-earth fluorescent and polymeric [79]. This synthetic technique involved the

fabrication of magnetic metallic nanocrystals at different reactions conditions. The reaction strategy is based upon the phase separation which occurs at the interface of solid–liquid–solution phases present in the reaction. For example the fabrication of monodisperse (6, 10 and 12 nm) Fe_3O_4 and MFe_2O_4 nanocrystals have been demonstrated by Sun *et al* and coworker [80].
Wuwei and co-worker have synthesized oblique and truncated nano cubes of α-Fe_2O_3 by one step facile hydrothermal method. This group studied the effect of volume ratio of oleylamine and acetylacetone for the fabrication of α-Fe_2O_3 with two different morphologies as shown in **Fig 6.3**. The synthesize magnetic nano particles were used for photocatalytic degradation of organic dye and it was observed that truncated nano cubes possess much higher photocatalytic degradation activity as compared to oblique nano cubes [81].

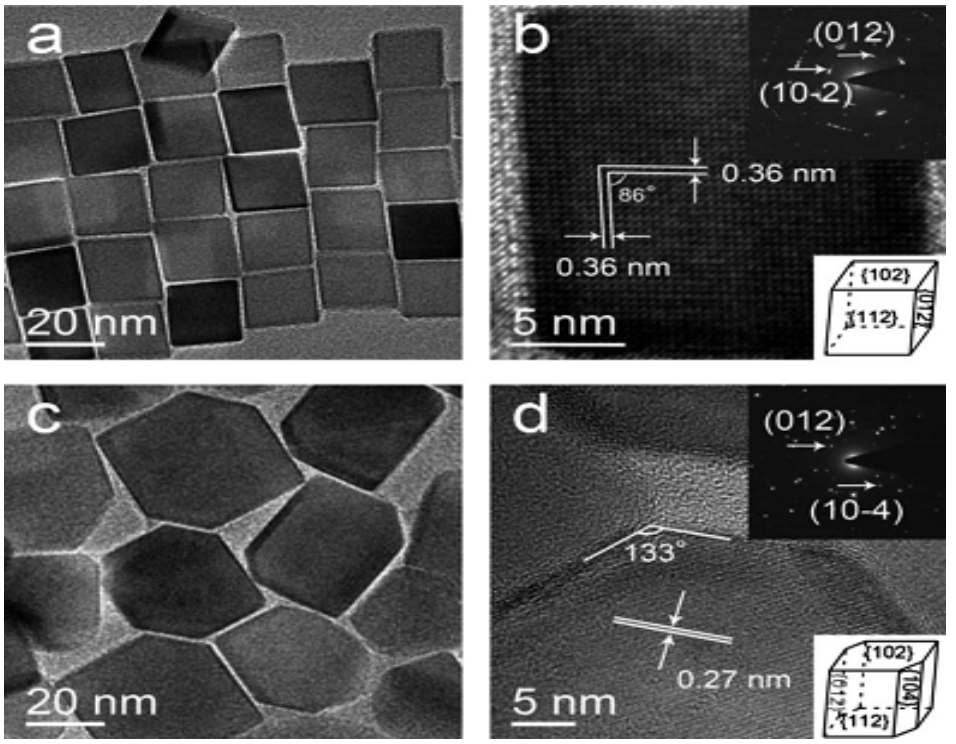

FIGURE 6.3
(a) TEM image of oblique nanocubes, (b) HRTEM image, FFT pattern and geometrical model of oblique nanocubes, (c) TEM image of truncated nanocubes, and (d) HRTEM image, FFT pattern and geometrical model of truncated nanocubes Reprinted from Ref [81]

The mechanism of formation of the α-Fe_2O_3 nanoparticles with oblique and truncated morphology is given below **scheme 2**. It was observed that the main cause of formation of two different morphologies is the presence of oleic acid. The presence of oleic acid led to the formation of oblique nano cubes whereas, truncated nano cubes are formed in the absence of oleic acid.

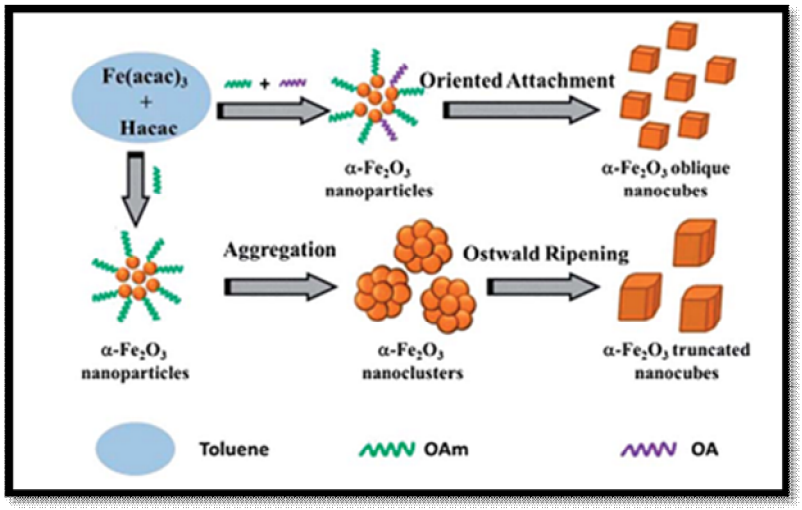

SCHEME 2
Mechanism of formation of oblique and truncated nano cubes. Reprinted from Ref [81]

Zeng *et al* and co-worker, have synthesized novel Fe_3O_4 nanoprism by a hydrothermal process using oleylamine (OAm) both as surfactant and reducing agent. The synthesized Fe_3O_4 exposed two kinds of crystal planes (111) and (220) as shown in **Fig 6.4**. [82].

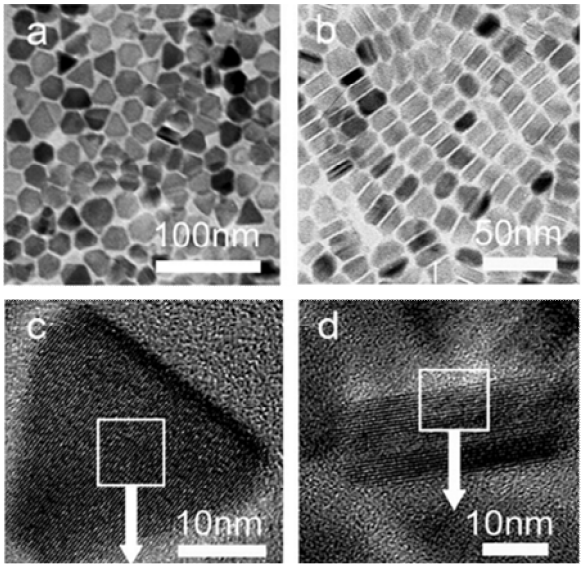

FIGURE 6.4
TEM images of Fe_3O_4 nanoprisms (a) lying flat and (b) self- assembled on the substrates (c, d) HRTEM images of Fe_3O_4 nanoprisms with a spacing of 0.301 nm Reprinted from Ref [82]

They experimentally proved the crystal plane dependent electrochemical activities of nanoprism as clear from **Fig 6.5** (b). Oleylamine was found to plays key role in the formation of different planes Fe_3O_4

nanoprism because the amine group of oleylamine absorb at certain planes and slows their growth while allowing the growth of other planes which leads to different morphology.

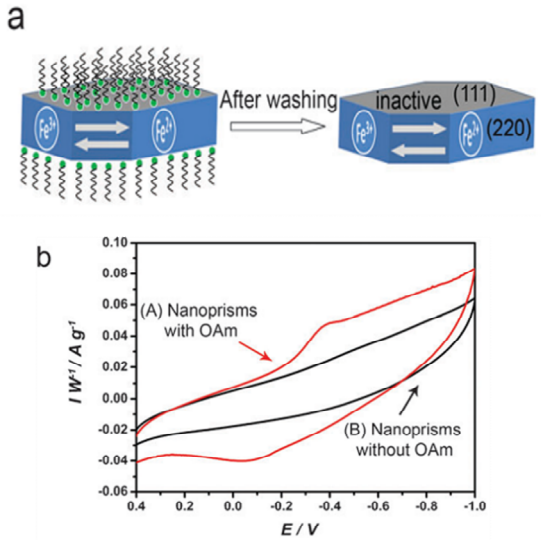

FIGURE 6.5
(a) Schematic illustration of Fe_3O_4 nanoprisms redox reaction. (b) Cyclic voltammograms of electrodes made of (A) Fe_3O_4 nanoprism with OAm (B) Fe_3O_4 nanoprisms without OAm in 1 M Na_2SO_3 Reprinted from Ref [82]

Microwave assisted synthesis

Microwave assisted method is a chemical method that use microwave radiation for heating materials containing electrical charges for instance polar molecule in the solvent or charge ion in the solid. As compared to the other heating methods microwave assisted solution fabrication methods have got more focus of research because of rapid processing, high reaction rate , reduce reaction time and high yield of product. Wang reported the synthesis of cubical spinal $M^{II}Fe_2O_4$ (M = Co, Mn, Ni) high crystalline structure in a short time of just 10 min by exposure the precursors to microwave radiation [83] shown in **Fig 6.6**. They have also used the microwave radiations for the synthesis of magnetite (Fe_3O_4) and hematite (α-Fe_2O_3).They have used $FeCl_3$, polyethylene glycol and $N_2H_4.H_2O$ as precursors and found that the amount of $N_2H_4.H_2O$ has a key role in controlling the final phase of Fe_3O_4 [84].

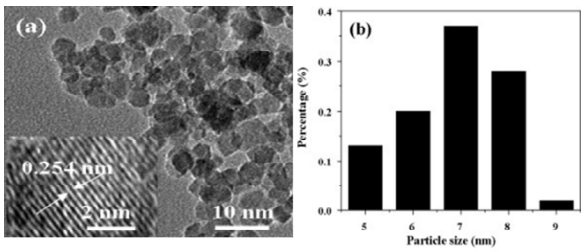

FIGURE 6.6
(a) TEM image of the $MnFe_2O_4$ and (b) the histogram showing particle size. Reprinted from Ref [84]

Presently, Swaminathan *et al* and co-worker have reported the facile synthesis of NdFeb nanoparticles using microwave radiations. Metal nitrate precursor were mixed with the glycine and then exposed to microwave radiation that led to the formation of Nd-Fe-B oxide which was further reduced by heating from 400 to 800 °C in the presence of CaH .The reduction started at 400°C, and at different temperatures different oxidation products can be identified. At 800 °C, the desired Nd_2 $Fe_{14}B$ phase along with alpha Fe and bi-product CaO phases are formed [85] **Fig 6.7** represent the different phases present in the XRD peak at different temperature..

Following reactions give the reduction of Nd Fe B oxide at 800 °C

$$7NdFeO_3 + 8Fe_3O_4 + 29FeO + NdBO_3 + B_2O_3 + 88CaH_2 \xrightarrow{800\ ^\circ C} 3Nd_2Fe14B + Nd2Fe17 + Fe + 88CaO + 176H_2$$

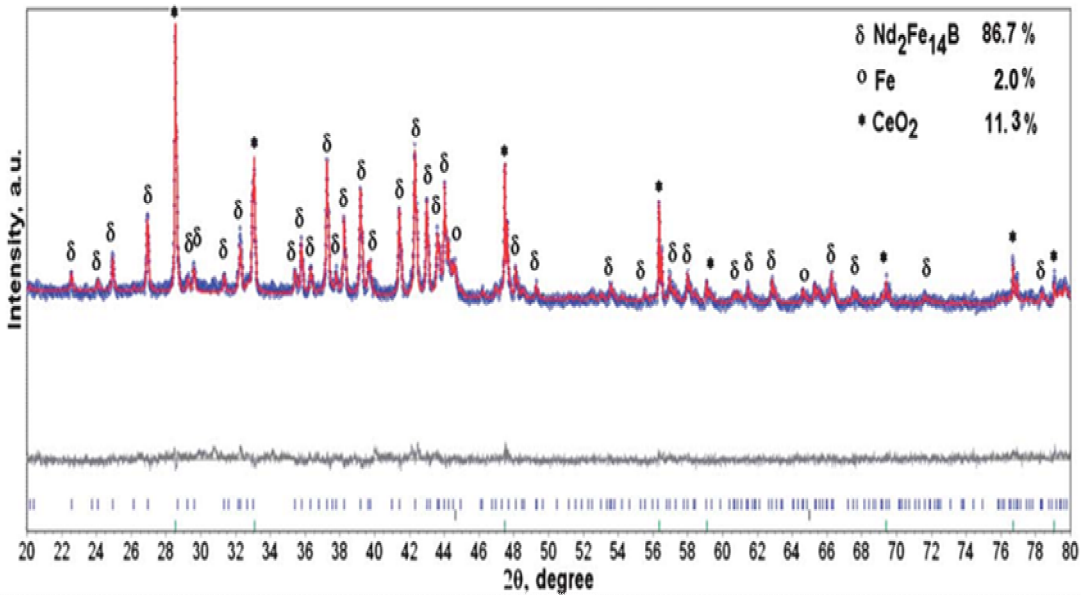

FIGURE 6.7
Rietveld refinement of Nd–Fe–B alloy synthesized by microwave reaction followed by reduction in the presence of CaH [85]

Template assisted fabrication

Another fabrication method used for the synthesis of magnetic nanoparticles, is the template-assisted fabrication [86]. The active template-based synthesis involves the growth of the nuclei at the holes and defects of the template. Subsequently the growth of the nuclei at the pre-formed template yields the desired morphology of the nanostructures. So through proper selection of base template, the size and shape of the magnetic nano particles can be controlled.

This technique has two important advantages over the chemical routes:

(i) Template use in the fabrication process determines the final size and morphology of the nanostructures.
(ii) Complex nanostructures such as nanobarcodes (segmented nanorods) nanoprism, nanocubes hexagons and octahedrons magnetic nano particles can be fabricated in an easy manner, with full control on size and morphology.

However, this method has also some drawback. It is a multi-step process that first of all required the fabrication base templates and then the subsequent deposition of magnetic material within the template. In the following discussion, we will highlight important recent progress that has been done in the template-assisted synthesis of complex magnetic nanostructures.
Mirkin *et al* and co-workers have demonstrated the synthesis of nanobarcodes (segmented nanowires with excellent control of composition along the length) of metals and polymers magnetic and non-magnetic materials. They demonstrated the fabrication of two component rod structure that was made by deposition of hydrophilic Au block and hydrophobic Polypyrrole block on anodic alumina oxide template. Due to the difference in the diameter of hydrophilic Au and hydrophobic Polypyrrole these sections were assembled in unique and exclusive pseudo-conical shape with three-dimensional bundle- and tubular-shaped structure as shown in Fig 6.8 [87].

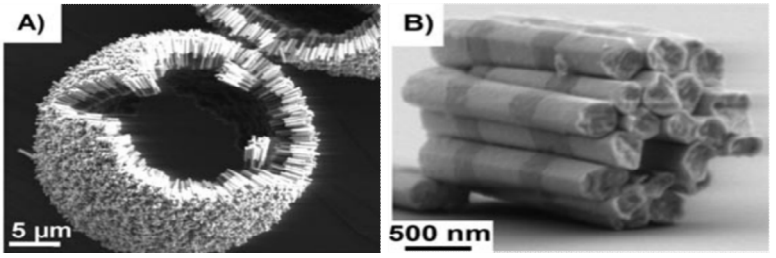

FIGURE 6.8
a) SEM image of self-assembly of Au-Polypyrrole rods into a tubular shape. b) SEM image showing the alignment of the ferromagnetic portion in a bundle of Au-Ni rods [87]

Recently, Han garter *et al*. have demonstrated the fabrication of multi component nanorods comprised of gold, nickel and poly-pyrrole [88]. **Fig 6.9** shows schematic over view of that fabrication of such segmented nanorods. In this method gold layer is sputterd on the alumina plate followed by deposition of material of interest into the pores of gold layer. For fabrication of nanorods (barcodes), the electro-deposition of the material is carried on, until a precise length is gained followed by the deposition of subsequent metal or polymer. Finally, the template is dissolved in the basic solution so as to remove the gold layer, and, to obtain the nanowires that can be functionalized or can be used for a wide number of applications.

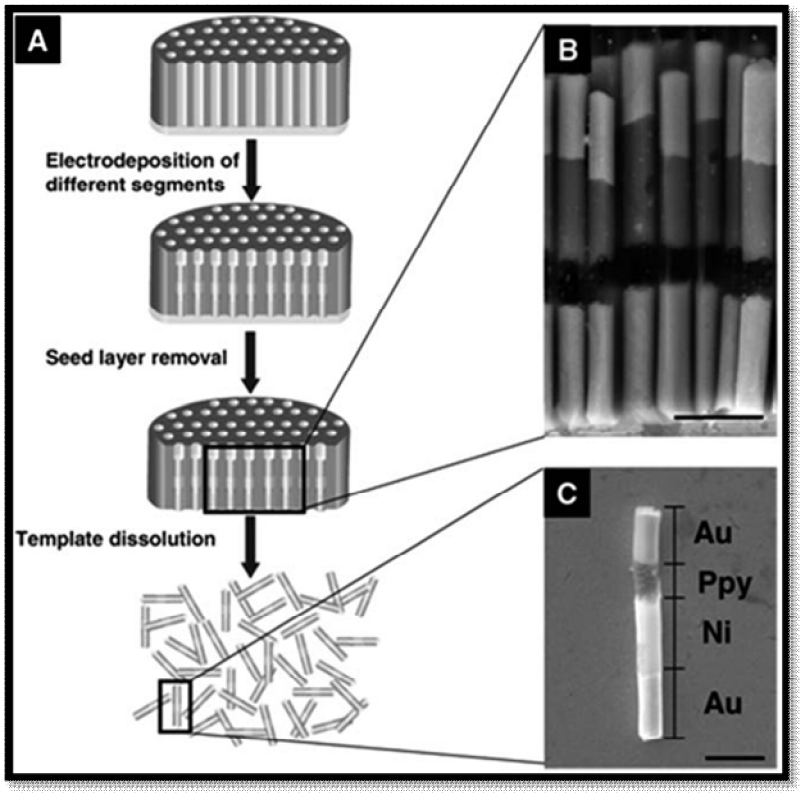

FIGURE 6.7
(a) Schematic representation of steps involved in the fabrication of multi segmented nanorods. (b) SEM image of the cross-section of segmented nanorods on the alumina template. (c) SEM image of single nanorod having different segments of the nanorods. (Scale bar ¼ 1 mm) reprinted from Ref [85]

Penner *et al* and co-workers have presented the fabrication of highly oriented nanowires of different metals e.g. Au, Ag, Cu, Pd, Ni and metal oxide (MoO_2) by using graphite template. This fabrication method involves the electrochemical deposition and nucleation of the magnetic nanoparticles at the step edges due to extreme low surface energy of the graphite template and relatively high activity of the step edges of metal nanoparticles [89, 90].Mann's group have used this technique for biomedical application using biomolecules as template [91, 92].

Tomoyuki *et al* and co-worker have demonstrated the fabrication of magnetic nanoparticle arrays by using diblock copolymer template substrate consisting of self-assembled polystyrene (PS) dots in a polymethylmethacrylate (PMMA) matrix and chemically synthesized Fe_3O_4 nanoparticles shown in Fig 6.8. This group studied the effect of dipping duration of the diblock copolymer template in the Fe_3O_4 solution, the withdrawal speed of the template from the solution and the volume fraction of Fe_3O_4 nanoparticles in the solution [93].

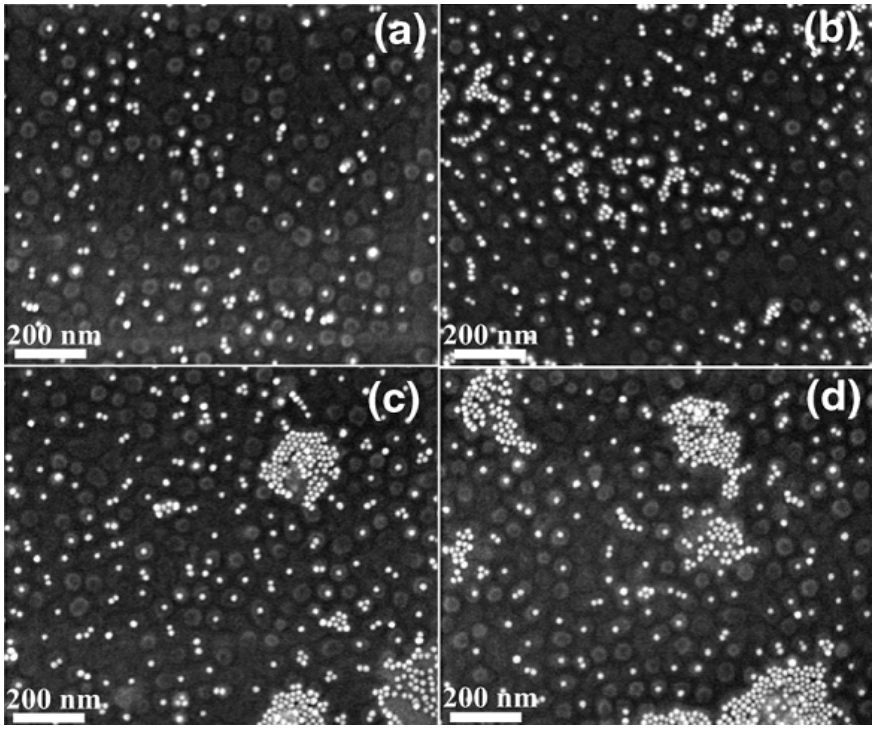

FIGURE 6.8
SEM images of Fe_3O_4 nanoparticles on self-assembled PS dots/PMMA matrix diblock copolymer template as a function of volume fraction of Fe_3O_4 nanoparticles in hexane for (a) 0.001 vol%, (b) 0.005 vol%, (c) 0.05 vol% and (d) 0.1 vol%, respectively reprinted from Ref [93]

Assembly of magnetic nanostructures

Self-assembly which is a ''bottom up'' nanofabrication approach involves thermodynamically atomic arrangements. This method involves the arrangements of molecules or magnetic nanoparticles into arrays of complex shape that are stabilized against destructive thermal decomposition via nanoscale forces. Self-assembly of nanoparticles can be obtained by application of nanostructured templates or external fields (field-directed or field-assisted assembly). Different strategies for assembly of magnetic nanostructures have been demonstrated. The functional superstructures like linear and branched chains and close packed arrays of magnetic nanostructures are formed due to relative strong dipole forces. Biological systems present the best examples of self-assembly of magnetic nanoparticles. Magnetite nanoparticle chains of 40–100 nm have been observed in magnetotactic bacteria. A permanent magnetic dipole that is critical for orientation of these bacteria, was resulted due to the chain-like assembly. There are numerous reports describing the spontaneous assembly of ferromagnetic nanoparticles into linear, branched chains and various other shapes. Singamaneni and Bliznyuk have exclusively demonstrated the self-assembly of magnetic nanoparticles through applying external magnetic field. They observed the formation of chains of Ni nanoparticles by application of the external magnetic field followed by evaporation of the solvents that give long interconnected chains of Ni nano particles. It was also observed that in the absence of external magnetic field, there was no

aggregation or chain like assembly results [94]. **Fig. 6.9** shows the AFM images of the self-assembly of Ni nanoparticles chains.

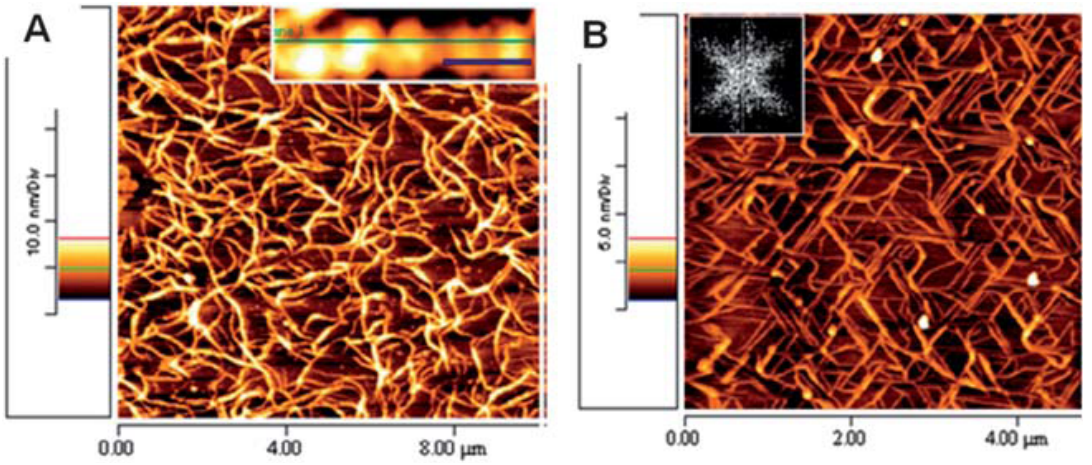

FIGURE 6.9
AFM images of self-assembled Ni nano chains formed in the presence of external magnetic field on (A) Image showing the array of nanoparticles connected to form a chain on silicon substrate and (B) highly oriented pyrolytic graphite reprinted from Ref [94]

Guided and template-assisted assembly

Template assisted fabrication is an attractive fabrication technique for magnetic nanostructures in which, not only the size, shape and composition of the nanostructures are controlled, but, it also allows the fabrication of pre-assembled structures. Park and co-workers have shown a unique approach for assembly of wide variety of magnetic, noble metals and semiconducting nanostructures into chains. They used anionic glycosaminoglycans, hyaluronic acid (HA) as a template, and the catechol was chemically introduced to the HA, called HA-catechol. It was proven that different types of nanoparticles were assembled onto linear HA-catechol. Nanoparticles solution concentration determines morphology and properties of the assemblies [95]. **Fig 6.10** shows show the ID assembly of the nanoparticles.
Sibener *et al* used polystyrene (PS)/poly (methyl methacrylate) (PMMA): PS-b- PMMA di-block-copolymer thin film as physical template for the assembly of FePt nanoparticles which resulted in a wide variety of patterns with nanoscale periodic structures.
Takahashi *et al* and co-workers have also presented the assembly of magnetic nano particles by using template substrate consisting of self-assembled polystyrene (PS) dots in Polymethylmethacrylate (PMMA) matrix [93].

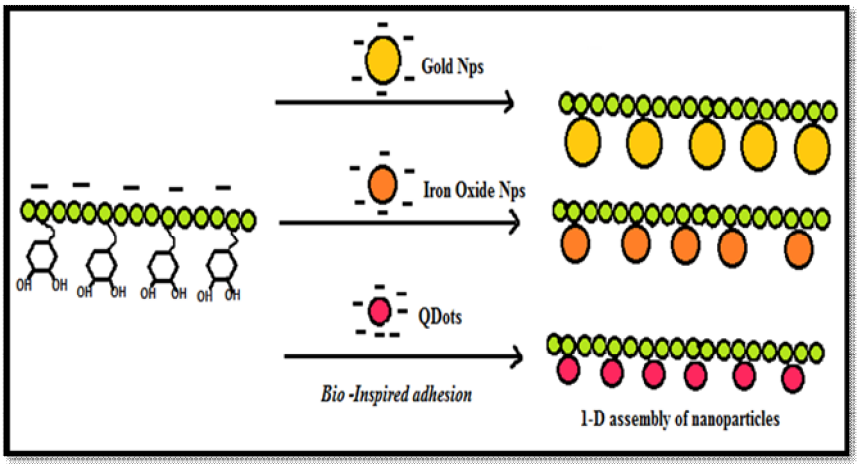

FIGURE 6.10
Schematic illustration of mussel-inspired, material-independent, 1D assembly of various nanoparticles reprinted from Ref [95]

Application of magnetic nanoparticles

Recent Advances in the biomedical applications of magnetic nano structures

Recently magnetic nano particles have been used for a wide number of applications, For example in industry, as magnetic inks for bank cheques and jet printing, high density magnetic data storage devices, magnetic information storage, xerography, catalysis, magnetic refrigeration, electronics (recording media) as photo catalyst for organic dye removal, for water splitting, gas sensors, as an electrode in Li-ion batteries in biomedical application and sewage treatment applications.

Because of the nano size of magnetic nano particles they can be attached to cell or they can be transported through the cell by introducing within the cell and can even directly enter into the blood stream. Biomedical applications are imposed to strict requirements on the particles (physical, chemical and pharmacological) properties, including chemical composition, size, granulometric uniformity, homogeneous crystal structure, magnetic properties, surface area and structure, adsorption properties, biocompatibility, hardness and flexibility, solubility, low toxicity and non-allergic affect. Numerous properties that offer abundant attractive possibilities to magnetic nanoparticles in biomedical field are their comparable sizes to those of a virus (20–500 nm), a protein (5–50 nm) or a gene (2 nm wide and 10–100 nm long) their superior magnetic properties and their large surface area that make them nontoxic, biocompatible and better suitable for biological system. In this chapter, we will only present the review of few applications of magnetic nanoparticles in biotechnology and energy applications.

Targeted drug delivery

Magnetic nanoparticles are used widely for drug targeting applications owing to its suitability. They can effectively and safely transfer the drug (with maximum loading) to a specific site. The following parameters of the nanomagnets are critical to be used as carriers for drug for, they possess smallest

particle size and large surface areas so that sedimentation time increases and the surface characteristics of magnetic nanoparticles protects them from degradation and make them excellent biocompatible drug delivery vehicles. They possess excellent magnetic properties to reduce the chances of nanomagnets concentration in blood and timely deliver the drug to the targeted side.
Several challenges associated with the application of the magnetic nanoparticles include their behavior in vivo systems. The efficiency in vivo applications before transfer to the target tissue, depends upon the ability of magnetic nanoparticles to cross biological barriers of the vascular endothelium or the blood brain barrier and the recognition and clearance by the reticulo-endothelial system (RES). Indirectly, the efficiency of magnetic nano particles is highly dependent on their size, morphology, charge and surface chemistry. Several techniques such as reducing size and grafting non-fouling polymers have been employed to increase the effectiveness of magnetic nanoparticles.
Next-generation magnetic nanoparticles for drug delivery incorporate novel nanocrystalline cores, coating materials and functional ligands to improve detection and specific delivery of the nanoparticles. New formulations of magnetic nano particles cores such as doped iron oxide nanocrystals, metallic/alloy nanoparticles and nanocomposites offer high magnetic moments increasing their signal-to-background ratios under MRI. Concurrently, the use of new surface coatings, such as stable gold or silica shell structures allows the application of otherwise toxic core materials as well as more thorough coating by formation of self-assembled monolayers (SAMS) on the nanoparticle surface.
Proteins [96], peptides, aptamers and small molecules [97] have been used as Targeting ligands to increase the site-specific accumulation of magnetic nanoparticles. In some cases some specific binding procedures are used to that stimulate internalization of the nanoparticle by receptor-mediated endocytosis. The following **scheme 3** shows the mechanism of targeted delivery of drug by magnetic nano particles to the tumour cell by receptor-mediated endocytosis. In this process the drug carrying magnetic nano particles are carried by blood stream to the specific tumour cells where they enter by formation of the endosome. Then endosome swells as a result of increase in osmotic pressure and finally ruptures to release the drug in the tumour cells.

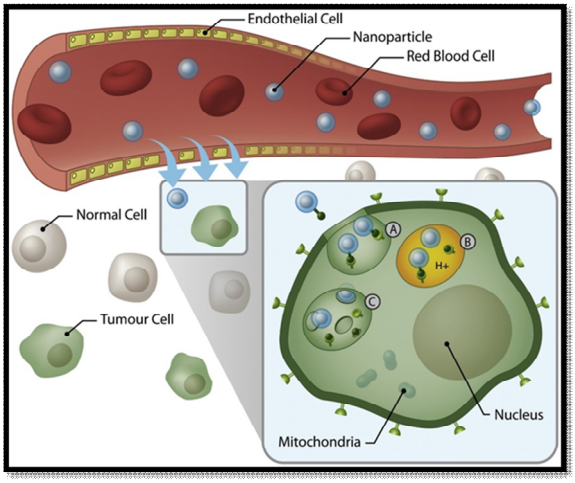

SCHEME 3
Illustration of tissue specific delivery of MNPs through active targeting facilitated by “leaky” vasculature. (A) Internalization of nanoparticles by (A) receptor-mediated endocytosis and formation of an endosome. (B) Endosomal acidification by proton pumps results in elevated osmotic pressure, swelling, and (C) rupture of the endosome allowing for release of the nanoparticle and conjugated therapeutic agents reprinted from Ref [98]

Haijuan *et al* and coworker have synthesized Fe_3O_4/SiO_2 hollow microspheres (HMS) with Fe_3O_4 as magnetic core and poly (ethylene glycol)-poly–(D,L-lactide) (PEG–PLA) as shell coating (HMS@PEG–PLA) for targeted drug delivery process. This ternary nanocomposite has advantages because of its hollow structure it can load a large quantity of drug ,due to magnetic properties it can easily be manipulated by application of applied external magnetic field and due to biodegradable and bioactive poly (ethylene glycol)-poly–(D,L-lactide) polymer coating it possesses biocompatibility [48]. The schematic for the synthesis hollow Fe_3O_4/SiO_2@PEG–PLA is given below in scheme 4.

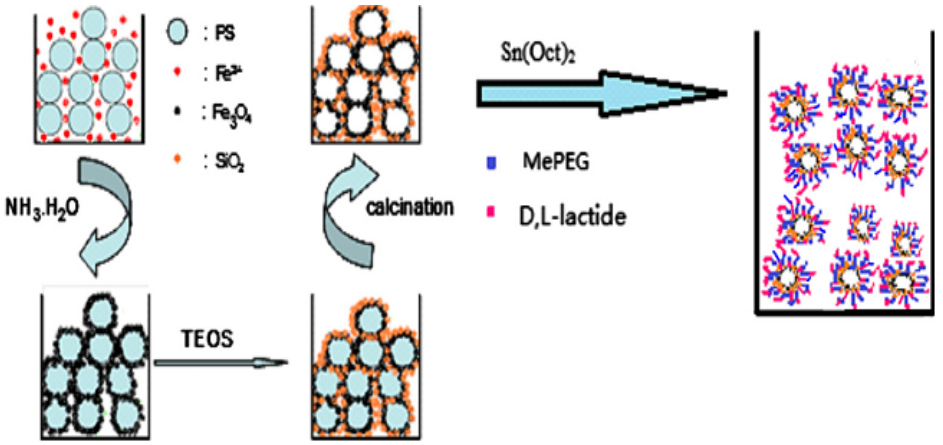

SCHEME 6.4
The synthesis procedure of hollow Fe_3O_4/SiO_2@PEG–PLA for controlled release of drug to the specific site reprinted from Ref [48]

In addition, recent studies and reviews show increasing role of cellular mechanics in diseases such as malaria and cancer metastasis. As such, there is a great potential for next-generation platforms to incorporate surface qualities that would enable probing and/or monitoring of local physical mechanistic changes at a length scale which would greatly assist in improving disease detection, monitoring, diagnosis, and treatment.

Nano magnetism in therapeutic hyperthermia

Magnetic nanoparticles are used for a wide range of clinical applications like targeted drug delivery, magnetic resonance imaging and magnetic fluid hyperthermia. Hyperthermia is one of the promising biomedical applications of magnetic nanoparticles for cancer treatment. Magnetic nanoparticle thermotherapy is the first heating technique that involves the use of magnetic nanoparticles for clinical application [99, 100]. Magnetic nanoparticles (nanosized magnets) act as thermal seeds in targeted magnetic hyperthermia treatment of cancers under an alternating magnetic field. Particles used for magnetically mediated hyperthermia include seeds such as rods of several mm size (1–300 mm) and nanoparticles (1–100 nm) [101, 102].The specific absorption rate (SAR) of the implant in an alternating magnetic field, reveals the heating rate. Thermal energy is then released to the surrounding of the targeted implant, varied with the size of the magnetic material used and the strength of the applied magnetic field [103].
In present clinical trials, a praiseworthy method of hyperthermia includes interstitial heating of targeted tumor cells followed by direct injection of magnetic nanoparticles to the targeted site. For

prostate cancer treatment, this clinical trial has been applied at two separate phase. The first phase is the applied magnetic nanoparticles thermotherapy alone, and, the second phase is the applied magnetics nanoparticle thermotherapy combination with permanent seed brachytherapy. As, with any other heating technique, this novel approach necessities specific tools for planning, quality control and thermal monitoring, based on appropriate imaging and modelling techniques [104-106].
Recently, multiphase magnetic composite materials have been successfully used to make effective tunable magnetic systems for treatment of hyperthermia to modify intrinsic magnetic properties, where the net contributions of different magnetic phases make it possible to modify the magnetization and anisotropy of the composite material [107, 108]. This approach involves for instance, mixed phase composites of $SrFe_{12}O_{19}/MgFe_2O_4/ZrO_2$ that have been prepared and, have efficient ability for the treatment of magnetic hyperthermia. The magnetic properties of hard/soft $SrFe_{12}O_{19}/NiFe_2O_4/ZnFe_2O_4$, $SrFe_{12}O_{19}/ZnFe_2O_4$ and $SrFe_{12}O_{19}/\gamma\text{-}Fe_2O_3$ composites have been studied [109]. The results conclude that exchange coupling between hard and soft phases, strongly, influences the magnetization and coercively of the composites.

Magnetic nano particles for Energy storage applications

Nowadays there is an urgent requirement to develop green and more efficient sources of energy. Most commonly used facile sources of energy are Li-ion batteries, fuel cell, supercapictors and hydrogen production cell. Lithium ion batteries that possess high charge and discharge ability, high energy density and high power capacity are the most efficient cost effective and attractive source of energy for power application and electric vehicles. These batteries have long been considered to be one of the most promising power sources for popular mobile devices, such as mobile phones, notebooks.
Magnetic nano particle also find application in this field [110]. Fe_3O_4 is one of the promising material that has been used as anode for lithium ions batteries [111-113], but, there are some drawbacks with Fe_3O_4 to use it as anode. For example it undergoes volume changes during the process of lithiation and de-lithiation, it possesses low conductivity that results in lower capacity and power cycalbility, which lowers the efficiency of the lithium ion batteries. To overcome these problems, Fe_3O_4 has been used as hybrid material with various other materials that enhance the properties of magnetic Fe_3O_4 and makes it suitable for the best performance in the batteries. For example, Jingshan *et al* and coworker have reported the atomic layer deposition of Fe_3O_4 nanocrystals on the 3-dimensional graphene foam for lithium ion batteries in which ZnO acts as sacrificial layer. This nanocomposite enhances the power capacity and energy density of Fe_3O_4 because three-dimensional (3D) graphene foam is extremely light and flexible as compared to other 3D bulk metal electrodes, and it possesses high electrical conductivity (around 1000 S/m) which ensures an efficient ion and electron transportation. Secondly, the bicontinuous Fe_3O_4 nanostructures are homogenously distributed on the graphene foam surface with a close physical contact that provides an efficient lithium ion and electron transport between Fe_3O_4 nanoparticles and 3D graphene foam, as well as transport ion between the electrolyte and the active material [114] as shown in **Fig 6.11**.

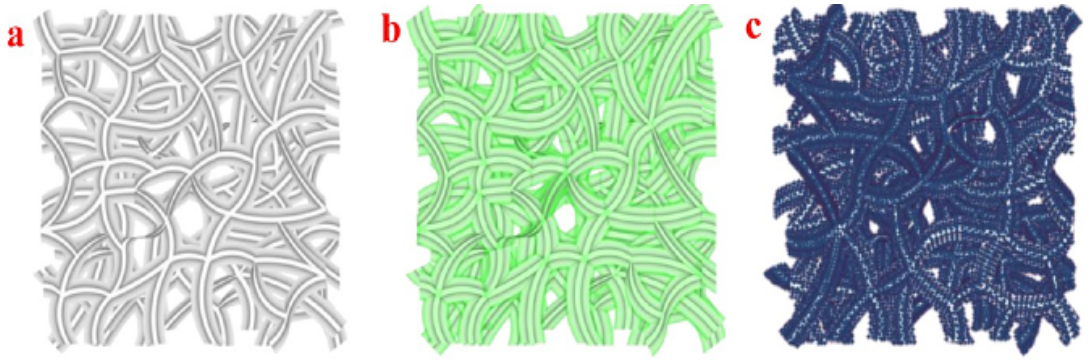

FIGURE 6.11
Schematic diagram of the sample structure. (a) Graphene foam backbone. (b) Graphene foam coated with ZnO by atomic layer deposition (GF@ZnO). (c) Graphene foam supported Fe_3O_4 nanostructure electrodes (GF@Fe_3O_4) reprinted from Ref [114]

The charge storage behavior of the GF@Fe_3O_4 electrodes was systematically investigated by cyclic voltammetry (CV). As shown in Figure 6.12a, in the first discharge process, two well defined reduction peaks can be resolved at 0.67 and 0.27 V respectively, corresponding to the structure transition induced by lithium intercalation (Fe_3O_4 + xLi+ + xe− → $LixFe_3O_4$) and the further, reduction of $LixFe_3O_4$ to Fe(0) by conversion reaction [LixFe3O4 +(8 − x)Li + +(8 − x)e− → 4Li2O + 3Fe]. As shown in the figure 6.12b, that cycling capacity of GF@Fe_3O_4 has been significantly increased as compared to pure GF.

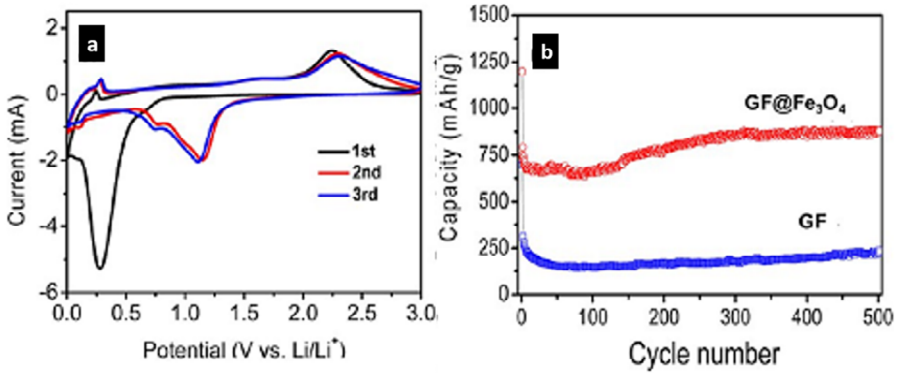

FIGURE 6.12
Electrochemical properties of the GF@Fe_3O_4 LIB electrodes. (a) CV curves of the GF@Fe_3O_4 electrode (b) Cycling profiles of the GF and GF@Fe_3O_4 electrodes at 1C rate, reprinted from Ref [38]

Recently Wang *et al* have used solvothermal method to construct a novel 3D monolith of Fe_2O_3/GS (graphene sheets) with high stability and Li storage ability. The monolith have 3D structure with interconnected macro porous framework with Fe_2O_3 nanocrystals. As shown in **Fig 6.13** interconnected macro porous structure, high conductivity and homogeneity of the structure results in excellent prolonged cycling stability of 733 mAh g^{-1} during 1000 charge/discharge cycles at 2000 mA g^{-1} [115].

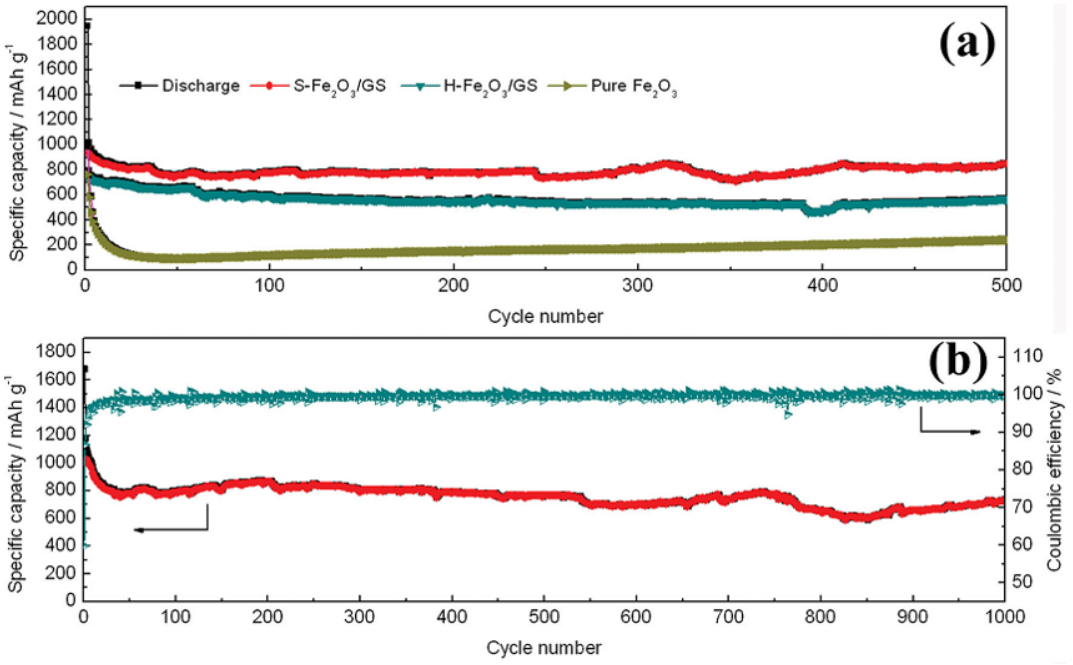

FIGURE 6.13
(a) Comparative cycle performance of S-Fe_2O_3 /GS, H-Fe_2O_3 /GS and pure Fe_2O_3 electrodes at a current density of 500 mA g^{-1}(b) cycle performance of S-Fe_2O_3 /GS at a current density of 2000 mA g^{-1} Reprinted from ref [115]

Conclusion

This chapter gives brief introduction of the applications and synthesis techniques use for the synthesis of magnetic nano particles. It explain that how to perform nano scale magnetism. Give an introduction about the various synthesis methods used for the preparation of well dispersed and isolated magnetic nanoparticles. Significantly the intensity of inter-particles interactions can dramatically affect the magnetic behavior of their macroscopic ensemble. We will have a look over the advances that have been happening in the synthesis and application of magnetic nanoparticles.

References

1. Lou, X.W., et al., *Self-Supported Formation of Needlelike Co3O4 Nanotubes and Their Application as Lithium-Ion Battery Electrodes.* Advanced Materials, 2008. **20**(2): p. 258-262.
2. Li, S., et al., *Vertically Aligned Carbon Nanotubes Grown on Graphene Paper as Electrodes in Lithium-Ion Batteries and Dye-Sensitized Solar Cells.* Advanced Energy Materials, 2011. **1**(4): p. 486-490.
3. Ye, J., et al., *Morphology-Controlled Synthesis of SnO2 Nanotubes by Using 1D Silica Mesostructures as Sacrificial Templates and Their Applications in Lithium-Ion Batteries.* Small, 2010. **6**(2): p. 296-306.

4. Wen, Z., et al., *Silicon nanotube anode for lithium-ion batteries.* Electrochemistry Communications, 2013. **29**: p. 67-70.
5. Liu, J., et al., *Direct growth of SnO 2 nanorod array electrodes for lithium-ion batteries.* Journal of Materials Chemistry, 2009. **19**(13): p. 1859-1864.
6. Song, Y., et al., *Large-scale porous hematite nanorod arrays: direct growth on titanium foil and reversible lithium storage.* The Journal of Physical Chemistry C, 2010. **114**(49): p. 21158-21164.
7. Yang, Z., et al., *Facile synthesis of CuO nanorod for lithium storage application.* Materials Letters, 2013. **90**: p. 4-7.
8. Wang, Z., S. Madhavi, and X.W. Lou, *Ultralong α-MoO3 Nanobelts: Synthesis and effect of binder choice on their lithium storage properties.* The Journal of Physical Chemistry C, 2012. **116**(23): p. 12508-12513.
9. Wang, H., et al., *Hollow Porous Silicon Oxide Nanobelts for High-Performance Lithium Storage.* Journal of Power Sources, 2014.
10. Mondal, A.K., et al., *Highly Porous NiCo2O4 Nanoflakes and Nanobelts as Anode Materials for Lithium-Ion Batteries with Excellent Rate Capability.* ACS applied materials & interfaces, 2014. **6**(17): p. 14827-14835.
11. Wang, L., et al., *Synthesis of Fe 3 O 4@ C core–shell nanorings and their enhanced electrochemical performance for lithium-ion batteries.* Nanoscale, 2013. **5**(9): p. 3627-3631.
12. Sun, J., et al., *Carbon nanorings and their enhanced lithium storage properties.* Advanced Materials, 2013. **25**(8): p. 1125-1130.
13. Nagaraju, G., *Ultra long single crystalline Na0. 3V2O5 nanofibers/nanorings synthesized by a facile one pot green approach and their lithium storage behavior.* Journal of the Brazilian Chemical Society, 2013. **24**(10): p. 1662-1668.
14. Zhang, B., et al., *Novel 3-D superstructures made up of SnO 2@ C core-shell nanochains for energy storage applications.* Chemical Communications, 2010. **46**(48): p. 9188-9190.
15. Bae, S.Y., et al., *Helical structure of single-crystalline ZnGa2O4 nanowires.* Journal of the American Chemical Society, 2005. **127**(31): p. 10802-10803.
16. Cui, R., Z. Han, and J.J. Zhu, *Helical carbon nanotubes: intrinsic peroxidase catalytic activity and its application for biocatalysis and biosensing.* Chemistry-A European Journal, 2011. **17**(34): p. 9377-9384.
17. Yang, P., et al., *Controlled growth of ZnO nanowires and their optical properties.* Advanced Functional Materials, 2002. **12**(5): p. 323.
18. Wang, X., et al., *Revealing the conversion mechanism of CuO nanowires during lithiation–delithiation by in situ transmission electron microscopy.* Chem. Commun., 2012. **48**(40): p. 4812-4814.
19. Qie, L., et al., *Nitrogen-Doped Porous Carbon Nanofiber Webs as Anodes for Lithium Ion Batteries with a Superhigh Capacity and Rate Capability.* Advanced Materials, 2012. **24**(15): p. 2047-2050.
20. Ji, L. and X. Zhang, *Evaluation of Si/carbon composite nanofiber-based insertion anodes for new-generation rechargeable lithium-ion batteries.* Energy & Environmental Science, 2010. **3**(1): p. 124-129.
21. Zhu, G.-N., et al., *Carbon-coated nano-sized Li 4 Ti 5 O 12 nanoporous micro-sphere as anode material for high-rate lithium-ion batteries.* Energy & Environmental Science, 2011. **4**(10): p. 4016-4022.
22. Cao, F.-F., et al., *Facile Synthesis of Mesoporous TiO2− C Nanosphere as an Improved Anode Material for Superior High Rate 1.5 V Rechargeable Li Ion Batteries Containing LiFePO4− C Cathode.* The Journal of Physical Chemistry C, 2010. **114**(22): p. 10308-10313.

23. Kim, J., et al., *Magnetic fluorescent delivery vehicle using uniform mesoporous silica spheres embedded with monodisperse magnetic and semiconductor nanocrystals.* Journal of the American Chemical Society, 2006. **128**(3): p. 688-689.
24. Schladt, T.D., et al., *Au@ MnO nanoflowers: hybrid nanocomposites for selective dual functionalization and imaging.* Angewandte Chemie International Edition, 2010. **49**(23): p. 3976-3980.
25. Wang, W. and H. Cui, *Chitosan-luminol reduced gold nanoflowers: from one-pot synthesis to morphology-dependent SPR and chemiluminescence sensing.* The Journal of Physical Chemistry C, 2008. **112**(29): p. 10759-10766.
26. Jia, F., et al., *Non-Aqueous Sol–Gel Approach towards the Controllable Synthesis of Nickel Nanospheres, Nanowires, and Nanoflowers.* Advanced Materials, 2008. **20**(5): p. 1050-1054.
27. Pawar, R., et al., *Growth of ZnO nanodisk, nanospindles and nanoflowers for gas sensor: pH dependency.* Current Applied Physics, 2012. **12**(3): p. 778-783.
28. Tang, Y., et al., *Hierarchical TiO2 nanoflakes and nanoparticles hybrid structure for improved photocatalytic activity.* The Journal of Physical Chemistry C, 2012. **116**(4): p. 2772-2780.
29. Zhang, X., et al., *Enhanced photoresponsive ultrathin graphitic-phase C3N4 nanosheets for bioimaging.* Journal of the American Chemical Society, 2012. **135**(1): p. 18-21.
30. Singamaneni, S., et al., *Magnetic nanoparticles: recent advances in synthesis, self-assembly and applications.* Journal of Materials Chemistry, 2011. **21**(42): p. 16819-16845.
31. Gao, J., H. Gu, and B. Xu, *Multifunctional magnetic nanoparticles: design, synthesis, and biomedical applications.* Accounts of chemical research, 2009. **42**(8): p. 1097-1107.
32. Xie, T., L. Xu, and C. Liu, *Synthesis and properties of composite magnetic material SrCo< sub> x</sub> Fe< sub> 12-x</sub> O< sub> 19</sub>(x= 0~ 0.3).* Powder Technology, 2012.
33. An, T., et al., *Synthesis of Carbon Nanotube–Anatase TiO2 Sub-micrometer-sized Sphere Composite Photocatalyst for Synergistic Degradation of Gaseous Styrene.* ACS applied materials & interfaces, 2012. **4**(11): p. 5988-5996.
34. Teymourian, H., A. Salimi, and S. Khezrian, *Fe< sub> 3</sub> O< sub> 4</sub> magnetic nanoparticles/reduced graphene oxide nanosheets as a novel electrochemical and bioeletrochemical sensing platform.* Biosensors and Bioelectronics, 2013.
35. Zhang, B., et al., *Microwave absorption enhancement of Fe3O4/polyaniline core/shell hybrid microspheres with controlled shell thickness.* Journal of Applied Polymer Science, 2013.
36. Rashad, M. and I. Ibrahim, *Structural, microstructure and magnetic properties of strontium hexaferrite particles synthesised by modified coprecipitation method.* Materials Technology: Advanced Performance Materials, 2012. **27**(4): p. 308-314.
37. Frey, N.A., et al., *Magnetic nanoparticles: synthesis, functionalization, and applications in bioimaging and magnetic energy storage.* Chemical Society Reviews, 2009. **38**(9): p. 2532-2542.
38. Ge, J., et al., *Superparamagnetic magnetite colloidal nanocrystal clusters.* Angewandte Chemie International Edition, 2007. **46**(23): p. 4342-4345.
39. Zhou, G., et al., *Graphene-wrapped Fe3O4 anode material with improved reversible capacity and cyclic stability for lithium ion batteries.* Chemistry of materials, 2010. **22**(18): p. 5306-5313.
40. Xu, H.L., Y. Shen, and H. Bi, *Reduced Graphene Oxide Decorated with Fe3O4 Nanoparticles as High Performance Anode for Lithium Ion Batteries.* Key Engineering Materials, 2012. **519**: p. 108-112.
41. Yoon, T., et al., *Electrostatic Self-Assembly of Fe3O4 Nanoparticles on Graphene Oxides for High Capacity Lithium-Ion Battery Anodes.* Energies, 2013. **6**(9): p. 4830-4840.

42. Wei, H., et al., *Preparation of Fe< sub> 3</sub> O< sub> 4</sub>@ graphene oxide core–shell magnetic particles for use in protein adsorption.* Materials Letters, 2012. **82**: p. 224-226.
43. Wu, Y., et al., *Conformal Fe3O4 Sheath on Aligned Carbon Nanotube Scaffolds as High-Performance Anodes for Lithium Ion Batteries.* Nano letters, 2013. **13**(2): p. 818-823.
44. Bychko, I., E.Y. Kalishin, and P. Strizhak, *Effect of the size of Fe@ Fe3O4 nanoparticles deposited on carbon nanotubes on their oxidation–reduction characteristics.* Theoretical and Experimental Chemistry, 2011. **47**(4): p. 219-224.
45. Liu, Z., et al., *Polyaniline-Coated Fe3O4 Nanoparticle–Carbon-Nanotube Composite and its Application in Electrochemical Biosensing.* Small, 2008. **4**(4): p. 462-466.
46. Sun, Y., et al., *Controlled Synthesis of Fe3O4/Ag Core–Shell Composite Nanoparticles with High Electrical Conductivity.* Journal of electronic materials, 2012. **41**(3): p. 519-523.
47. Zhao, R., et al., *Hierarchically nanostructured Fe< sub> 3</sub> O< sub> 4</sub> microspheres and their novel microwave electromagnetic properties.* Materials Letters, 2010. **64**(3): p. 457-459.
48. Deng, H. and Z. Lei, *Preparation and characterization of hollow Fe< sub> 3</sub> O< sub> 4</sub>/SiO< sub> 2</sub>@ PEG-PLA nanoparticles for drug delivery.* Composites Part B: Engineering, 2013.
49. Sun, J., et al., *Synthesis and characterization of biocompatible Fe3O4 nanoparticles.* Journal of Biomedical Materials Research Part A, 2007. **80**(2): p. 333-341.
50. Liu, Z., et al., *Single crystalline magnetite nanotubes.* Journal of the American Chemical Society, 2005. **127**(1): p. 6-7.
51. Zhong, Z., et al., *A versatile wet-chemical method for synthesis of one-dimensional ferric and other transition metal oxides.* Chemistry of materials, 2006. **18**(25): p. 6031-6036.
52. Jiao, F., et al., *Synthesis of ordered mesoporous Fe3O4 and γ-Fe2O3 with crystalline walls using post-template reduction/oxidation.* Journal of the American Chemical Society, 2006. **128**(39): p. 12905-12909.
53. Du, N., et al., *Selective synthesis of Fe2O3 and Fe3O4 nanowires via a single precursor: a general method for metal oxide nanowires.* Nanoscale research letters, 2010. **5**(8): p. 1295-1300.
54. Wang, G., et al., *The synthesis of magnetic and fluorescent bi-functional silica composite nanoparticles via reverse microemulsion method.* Journal of fluorescence, 2009. **19**(6): p. 939-946.
55. Jin, J., S.i. Ohkoshi, and K. Hashimoto, *Giant coercive field of nanometer-sized iron oxide.* Advanced Materials, 2004. **16**(1): p. 48-51.
56. Han, Y.C., et al., *Synthesis of highly magnetized iron nanoparticles by a solventless thermal decomposition method.* The Journal of Physical Chemistry C, 2007. **111**(17): p. 6275-6280.
57. Sun, S. and H. Zeng, *Size-controlled synthesis of magnetite nanoparticles.* Journal of the American Chemical Society, 2002. **124**(28): p. 8204-8205.
58. Kang, M., *Synthesis of Fe/TiO< sub> 2</sub> photocatalyst with nanometer size by solvothermal method and the effect of H< sub> 2</sub> O addition on structural stability and photodecomposition of methanol.* Journal of Molecular Catalysis A: Chemical, 2003. **197**(1): p. 173-183.
59. Ai, L., C. Zhang, and Z. Chen, *Removal of methylene blue from aqueous solution by a solvothermal-synthesized graphene/magnetite composite.* Journal of hazardous materials, 2011. **192**(3): p. 1515-1524.
60. Park, J., et al., *Ultra-large-scale syntheses of monodisperse nanocrystals.* Nature materials, 2004. **3**(12): p. 891-895.

61. Teja, A.S. and P.-Y. Koh, *Synthesis, properties, and applications of magnetic iron oxide nanoparticles.* Progress in Crystal Growth and Characterization of Materials, 2009. **55**(1): p. 22-45.
62. Guo, Q., et al., *Patterned Langmuir-Blodgett films of monodisperse nanoparticles of iron oxide using soft lithography.* Journal of the American Chemical Society, 2003. **125**(3): p. 630-631.
63. Taniguchi, I., *Powder properties of partially substituted LiM< sub> x</sub> Mn< sub> 2− x</sub> O< sub> 4</sub>(M= Al, Cr, Fe and Co) synthesized by ultrasonic spray pyrolysis.* Materials Chemistry and Physics, 2005. **92**(1): p. 172-179.
64. Dosev, D., et al., *Magnetic/luminescent core/shell particles synthesized by spray pyrolysis and their application in immunoassays with internal standard.* Nanotechnology, 2007. **18**(5): p. 055102.
65. Zhong, L.S., et al., *Self-Assembled 3D flowerlike iron oxide nanostructures and their application in water treatment.* Advanced Materials, 2006. **18**(18): p. 2426-2431.
66. Polshettiwar, V., B. Baruwati, and R.S. Varma, *Self-assembly of metal oxides into three-dimensional nanostructures: synthesis and application in catalysis.* ACS Nano, 2009. **3**(3): p. 728-736.
67. Jia, C.-J., et al., *Large-scale synthesis of single-crystalline iron oxide magnetic nanorings.* Journal of the American Chemical Society, 2008. **130**(50): p. 16968-16977.
68. Li, Z., et al., *One-Pot Reaction to Synthesize Biocompatible Magnetite Nanoparticles.* Advanced Materials, 2005. **17**(8): p. 1001-1005.
69. Jia, C.J., et al., *Single-Crystalline Iron Oxide Nanotubes.* Angewandte Chemie, 2005. **117**(28): p. 4402-4407.
70. Jana, N.R., Y. Chen, and X. Peng, *Size-and shape-controlled magnetic (Cr, Mn, Fe, Co, Ni) oxide nanocrystals via a simple and general approach.* Chemistry of materials, 2004. **16**(20): p. 3931-3935.
71. Rockenberger, J., E.C. Scher, and A.P. Alivisatos, *A new nonhydrolytic single-precursor approach to surfactant-capped nanocrystals of transition metal oxides.* Journal of the American Chemical Society, 1999. **121**(49): p. 11595-11596.
72. Zeng, H., et al., *Exchange-coupled nanocomposite magnets by nanoparticle self-assembly.* Nature, 2002. **420**(6914): p. 395-398.
73. Salazar-Alvarez, G., et al., *Cubic versus spherical magnetic nanoparticles: the role of surface anisotropy.* Journal of the American Chemical Society, 2008. **130**(40): p. 13234-13239.
74. Zhang, H., et al., *Engineering magnetic properties of Ni nanoparticles by non-magnetic cores.* Chemistry of materials, 2009. **21**(21): p. 5222-5228.
75. Adschiri, T., et al., *Hydrothermal synthesis of metal oxide nanoparticles at supercritical conditions.* Journal of Nanoparticle Research, 2001. **3**(2-3): p. 227-235.
76. Yu, J. and X. Yu, *Hydrothermal synthesis and photocatalytic activity of zinc oxide hollow spheres.* Environmental science & technology, 2008. **42**(13): p. 4902-4907.
77. Yang, T., et al., *Room-temperature ferromagnetic Mn-doped ZnO nanocrystal synthesized by hydrothermal method under high magnetic field.* Materials Science and Engineering: B, 2010. **170**(1): p. 129-132.
78. Hu, J. and Y. Bando, *Growth and optical properties of single-crystal tubular ZnO whiskers.* Applied Physics Letters, 2003. **82**(9): p. 1401-1403.
79. Wang, X., et al., *A general strategy for nanocrystal synthesis.* Nature, 2005. **437**(7055): p. 121-124.
80. Sun, S., et al., *Monodisperse MFe2O4 (M= Fe, Co, Mn) nanoparticles.* Journal of the American Chemical Society, 2004. **126**(1): p. 273-279.

81. Wu, W., et al., *Single-crystalline α-Fe2O3 nanostructures: controlled synthesis and high-index plane-enhanced photodegradation by visible light.* J. Mater. Chem. A, 2013. **1**(23): p. 6888-6894.
82. Zeng, Y., et al., *One-pot synthesis of Fe3O4 nanoprisms with controlled electrochemical properties.* Chemical Communications, 2010. **46**(22): p. 3920-3922.
83. Wang, W.-W., *Microwave-induced polyol-process synthesis of M< sup> II</sup> Fe< sub> 2</sub> O< sub> 4</sub>(M= Mn, Co) nanoparticles and magnetic property.* Materials Chemistry and Physics, 2008. **108**(2): p. 227-231.
84. Wang, W.-W., Y.-J. Zhu, and M.-L. Ruan, *Microwave-assisted synthesis and magnetic property of magnetite and hematite nanoparticles.* Journal of Nanoparticle Research, 2007. **9**(3): p. 419-426.
85. Swaminathan, V., et al., *Novel microwave assisted chemical synthesis of Nd2Fe14B hard magnetic nanoparticles.* Nanoscale, 2013. **5**(7): p. 2718-2725.
86. Sander, D., et al., *New insights into nano-magnetism by spin-polarized scanning tunneling microscopy.* Journal of Electron Spectroscopy and Related Phenomena, 2012.
87. Hurst, S.J., et al., *Multisegmented One-Dimensional Nanorods Prepared by Hard-Template Synthetic Methods.* Angewandte Chemie International Edition, 2006. **45**(17): p. 2672-2692.
88. Hangarter, C.M., et al., *Conducting polymer nanowires for chemiresistive and FET-based bio/chemical sensors.* Journal of Materials Chemistry, 2010. **20**(16): p. 3131-3140.
89. Penner, R.M., *Mesoscopic metal particles and wires by electrodeposition.* The Journal of Physical Chemistry B, 2002. **106**(13): p. 3339-3353.
90. Atashbar, M.Z., D. Banerji, and S. Singamaneni, *Room-temperature hydrogen sensor based on palladium nanowires.* Sensors Journal, IEEE, 2005. **5**(5): p. 792-797.
91. Wong, K.K. and S. Mann, *Biomimetic synthesis of cadmium sulfide-ferritin nanocomposites.* Advanced Materials, 1996. **8**(11): p. 928-932.
92. Wong, K.K., et al., *Biomimetic synthesis and characterization of magnetic proteins (magnetoferritin).* Chemistry of materials, 1998. **10**(1): p. 279-285.
93. Ogawa, T., et al., *Fabrication of Fe3O4 nanoparticle arrays via patterned template assisted self-assembly.* Nanotechnology, 2006. **17**(22): p. 5539.
94. Zeng, H., et al., *Shape-controlled synthesis and shape-induced texture of MnFe2O4 nanoparticles.* Journal of the American Chemical Society, 2004. **126**(37): p. 11458-11459.
95. Lee, Y., et al., *A Bioinspired Polymeric Template for 1D Assembly of Metallic Nanoparticles, Semiconductor Quantum Dots, and Magnetic Nanoparticles.* Macromolecular rapid communications, 2010. **31**(24): p. 2109-2114.
96. Kresse, M., et al., *Targeting of ultrasmall superparamagnetic iron oxide (USPIO) particles to tumor cells in vivo by using transferrin receptor pathways.* Magnetic Resonance in Medicine, 1998. **40**(2): p. 236-242.
97. McCarthy, J.R. and R. Weissleder, *Multifunctional magnetic nanoparticles for targeted imaging and therapy.* Advanced drug delivery reviews, 2008. **60**(11): p. 1241-1251.
98. Sun, C., J.S. Lee, and M. Zhang, *Magnetic nanoparticles in MR imaging and drug delivery.* Advanced drug delivery reviews, 2008. **60**(11): p. 1252-1265.
99. Johannsen, M., et al., *Clinical hyperthermia of prostate cancer using magnetic nanoparticles: presentation of a new interstitial technique.* International journal of hyperthermia, 2005. **21**(7): p. 637-647.
100. Sonvico, F., et al., *Folate-conjugated iron oxide nanoparticles for solid tumor targeting as potential specific magnetic hyperthermia mediators: synthesis, physicochemical characterization, and in vitro experiments.* Bioconjugate chemistry, 2005. **16**(5): p. 1181-1188.

101.Thiesen, B. and A. Jordan, *Clinical applications of magnetic nanoparticles for hyperthermia.* International journal of hyperthermia, 2008. **24**(6): p. 467-474.
102.Khot, V., et al., *Induction heating studies of dextran coated MgFe 2 O 4 nanoparticles for magnetic hyperthermia.* Dalton Transactions, 2013. **42**(4): p. 1249-1258.
103.Martinez-Boubeta, C., et al., *Learning from nature to improve the heat generation of iron-oxide nanoparticles for magnetic hyperthermia applications.* Sci Rep, 2013. **3**.
104.Etheridge, M.L., et al., *Accounting for biological aggregation in heating and imaging of magnetic nanoparticles.* Technology, 2014. **2**(03): p. 214-228.
105.Liu, Y., et al., *Facile Surface Functionalization of Hydrophobic Magnetic Nanoparticles.* Journal of the American Chemical Society, 2014. **136**(36): p. 12552-12555.
106.Simeonidis, K., et al., *Fe-based nanoparticles as tunable magnetic particle hyperthermia agents.* Journal of Applied Physics, 2013. **114**(10): p. 103904.
107.Branquinho, L.C., et al., *Effect of magnetic dipolar interactions on nanoparticle heating efficiency: Implications for cancer hyperthermia.* Sci Rep, 2013. **3**.
108.Salas, G., S. Veintemillas-Verdaguer, and M.d.P. Morales, *Relationship between physico-chemical properties of magnetic fluids and their heating capacity.* International journal of hyperthermia, 2013. **29**(8): p. 768-776.
109.Ur Rashid, A., et al., *Strontium Hexaferrite (SrFe< sub> 12</sub> O< sub> 19</sub>) Based Composites for Hyperthermia Applications.* Journal of Magnetism and Magnetic Materials, 2013.
110.Zhang, L., et al., *Formation of Fe2O3 Microboxes with Hierarchical Shell Structures from Metal–Organic Frameworks and Their Lithium Storage Properties.* Journal of the American Chemical Society, 2012. **134**(42): p. 17388-17391.
111.Du, N., et al., *Layer-by-layer synthesis of γ-Fe 2 O 3@ SnO 2@ C porous core–shell nanorods with high reversible capacity in lithium-ion batteries.* Nanoscale, 2013. **5**(11): p. 4744-4750.
112.Yan, Y., et al., *Large-scale facile synthesis of Fe-doped SnO 2 porous hierarchical nanostructures and their enhanced lithium storage properties.* Journal of Materials Chemistry A, 2014. **2**(38): p. 15875-15882.
113.Han, S., et al., *One-Step Hydrothermal Synthesis of 2D Hexagonal Nanoplates of α-Fe2O3/Graphene Composites with Enhanced Photocatalytic Activity.* Advanced Functional Materials, 2014. **24**(36): p. 5719-5727.
114.Luo, J., et al., *3D Graphene Foam Supported Fe3O4 Lithium Battery Anodes with Long Cycle Life and High Rate Capability.* Nano letters, 2013.
115.Wang, R., et al., *Solvothermal-Induced Self-Assembly of Fe2O3/GS Aerogels for High Li-Storage and Excellent Stability.* Small, 2014.